Faculty Authored Articles

2004

A Computational Model for Martensitic Thin Films With Compositional Fluctuation

Pavel Bělík
Augsburg University, belik@augsburg.edu

Mitchell Luskin
University of Minnesota - Twin Cities

A COMPUTATIONAL MODEL FOR MARTENSITIC THIN FILMS WITH COMPOSITIONAL FLUCTUATION

PAVEL BĚLÍK AND MITCHELL LUSKIN

ABSTRACT. We develop a computational model for the martensitic first-order structural phase transformation in a single crystal thin film, and we use this model to study the effect of spatial compositional fluctuation, spatial temporal noise, and the loss of stability of the metastable phase at temperatures sufficiently far from the transformation temperature.

1. INTRODUCTION

We developed in [5] a computational model for the phase transformation of a single crystal thin film from a stress-free indented martensitic shape to a flat austenitic shape as the film is heated. In the computational model, the indented film transformed quasi-statically through a sequence of metastable states (local minima) for the elastic free energy while the temperature field evolved dynamically. Since the indented shape was a metastable state for all temperatures, we introduced into the algorithm a Monte Carlo nucleation procedure based on a temperature-dependent probability distribution function.

In our computations, the indentation shrank in size, but remained tent-like. In the experiment of Cui and James [9], though, the indentation initially shrank through a sequence of smaller tent-like shapes, but the indentation eventually rounded. We also presented computations in [5] with a "relaxed" energy density, but in this case the indentation immediately relaxed to a rounded shape since the relaxation removed the barriers to the formation of energy-reducing microstructure. In this paper, we consider several modifications to the thin film computational model to more closely simulate the shape of the transforming indentation in the experiment as well as to more generally explore the effects of compositional variation, spatial temporal noise, and the loss of stability of the metastable phase.

We modify the elastic free energy density to account for compositional disorder. The transformation temperature of martensitic crystals can have a strong dependence on the composition of its alloy constituents [8, 10, 11, 15]. Since the composition of martensitic alloys can exhibit spatial fluctuation, the phase transformation behavior of such alloys can be expected to depend significantly on the coupling between the compositional variation and the strong dependence of the transformation temperature on composition. The transformation temperature of our modified free energy density is an independent Gaussian random variable $\theta_c|_K$ indexed by the triangles K in the finite element mesh. Regions with a low local transformation temperature will likely serve as sites of nucleation of

austenite when heating the crystal and regions of high local transformation temperature will likely serve as sites of nucleation of martensite when cooling the material.

The martensitic phase was a metastable state for the elastic free energy density used for the computations in [5] for all temperatures above the transformation temperature. For this reason, we needed to include a nucleation step in the algorithm used in [5] to make the transformation to the austenitic phase possible as the film was heated. In this paper, we also modify the elastic free energy density to allow the loss of metastability of the martensitic phase at sufficiently large temperatures, and we study the effect of this modification on the phase transformation and on the evolution of the transforming indentation.

We finally consider the effect of adding independent random Gaussian perturbations to the deformation at each time step and on each spatial finite element triangle. These perturbations can model the effect of vibrations in the operating environment of the active thin film.

2. The Free Energy Density

In order to incorporate compositional variation into the model, we shall modify the free energy density used in the geometrically nonlinear theory for martensite [1, 2, 12, 13]. The composition-dependent free energy density $\phi(F, \theta, c)$ is a continuous function $\phi : \mathbb{R}^{3\times 3} \times (\theta_0, \theta_1) \times [0, 1] \to \mathbb{R}$ representing the free energy per unit reference volume of the material as a function of the deformation gradient $F \in \mathbb{R}^{3\times 3}$, the temperature $\theta \in (\theta_0, \theta_1)$, and a compositional order parameter $c \in [0, 1]$. Since the transformation temperature θ_c can be expected to depend monotonically and continuously on the composition c, it will be convenient to denote the energy density as a function of transformation temperature θ_c rather than composition c, so we will use the notation $\phi = \phi(F, \theta, \theta_c)$ for $F \in \mathbb{R}^{3\times 3}$ and $\theta, \theta_c \in (\theta_0, \theta_1)$.

In addition to the properties above, we assume that the free energy density ϕ is frame-indifferent and satisfies the material symmetry imposed by the symmetry of the austenitic crystalline lattice. The frame-indifference is mathematically expressed by the condition

$$\phi(RF, \theta, \theta_c) = \phi(F, \theta, \theta_c) \quad \text{for all } R \in \mathrm{SO}(3), \ F \in \mathbb{R}^{3\times 3}, \text{ and } \ \theta, \theta_c \in (\theta_0, \theta_1),$$

where $\mathrm{SO}(3)$ denotes the group of proper rotations. The material symmetry is expressed by

$$\phi(FR, \theta, \theta_c) = \phi(F, \theta, \theta_c) \quad \text{for all } R \in \mathcal{G}, \ F \in \mathbb{R}^{3\times 3}, \text{ and } \ \theta, \theta_c \in (\theta_0, \theta_1),$$

where $\mathcal{G} \subset \mathrm{SO}(3)$ is the symmetry group of the austenitic crystalline lattice.

In order to model the phase transformation when the temperature, θ, varies through the transformation temperature, θ_c, we shall assume that the free energy density, $\phi(F, \theta, \theta_c)$, as a function of the deformation gradient $F \in \mathbb{R}^{3\times 3}$ at fixed temperatures $\theta \geq \theta_c$ is minimized on $\mathrm{SO}(3)$. We note that this assumption neglects the possible thermal expansion of the austenitic phase. We also assume that the transformation strain U_1 for the unstressed martensitic phase does not vary with temperature, so that the free energy density as a function of $F \in \mathbb{R}^{3\times 3}$ for fixed temperatures $\theta \leq \theta_c$ is minimized on

$$\mathcal{U} = \mathrm{SO}(3)U_1 \cup \cdots \cup \mathrm{SO}(3)U_N,$$

where for the symmetry group $\mathcal{G}$ of the austenitic phase we have that the martensitic variants are given by

$$\{U_1, \ldots, U_N\} = \{R^T U_1 R : \ R \in \mathcal{G}\}.$$

We will consider a CuZnAl alloy that undergoes a cubic-to-monoclinic transformation and thus has twelve ($N = 12$) variants. However, we will use an energy density that is minimized only at the

wells with the maximal in-plane extensions generated by the four variants U_i, $i = 1, \ldots, 4$, given by

$$U_1 = \begin{pmatrix} \alpha & \delta & 0 \\ \delta & \beta & 0 \\ 0 & 0 & \gamma \end{pmatrix}, \quad U_2 = \begin{pmatrix} \beta & \delta & 0 \\ \delta & \alpha & 0 \\ 0 & 0 & \gamma \end{pmatrix}, \quad U_3 = \begin{pmatrix} \alpha & -\delta & 0 \\ -\delta & \beta & 0 \\ 0 & 0 & \gamma \end{pmatrix}, \quad U_4 = \begin{pmatrix} \beta & -\delta & 0 \\ -\delta & \alpha & 0 \\ 0 & 0 & \gamma \end{pmatrix}, \quad (2.1)$$

with $\alpha, \beta, \gamma, \delta > 0$, $\alpha > \beta$, and $\alpha\beta - \delta^2 > 0$ [3, 5]. The parameters for Cu-Zn(at.%)15-Al(at.%)17 are [3, 7]

$$\alpha = 1.087, \quad \beta = 1.01, \quad \gamma = 0.9093, \quad \delta = 0.025.$$

When $\theta = \theta_c$, the free energy density is minimized by both the austenite and martensite. Near the transformation temperature, both phases remain local minimizers of ϕ. In this paper, we shall modify the free energy density in [5] to study the effect of the loss of stability of local minimizers of the free energy density at temperatures sufficiently far from the transformation temperature.

We use the energy densities $W_M(F)$ for the martensitic phase and $W_A(F)$ for the austenitic phase given in [3] such that

$$W_M(F) = 0 \quad \text{if and only if} \quad F \in \mathcal{U} = \mathrm{SO}(3)U_1 \cup \cdots \cup \mathrm{SO}(3)U_4,$$
$$W_A(F) = 0 \quad \text{if and only if} \quad F \in \mathrm{SO}(3),$$

where the $W_M(F)$ and $W_A(F)$ approximately match the elastic moduli at their respective energy wells.

To allow the metastable phases to lose stability at temperatures sufficiently far from the transformation temperature, we extend the energy density given in [5] to

$$\phi(F, \theta, \theta_c) = \begin{cases} \min\left\{ W_A(F), \; W_M(F) + C_A \cdot \frac{(\theta - \theta_c)W_A(U_1)}{W_A(U_1) + (\theta - \theta_c)} \right\} & \text{for } \theta \geq \theta_c, \\ \min\left\{ W_A(F) + C_M \cdot \frac{(\theta_c - \theta)W_M(I)}{W_M(I) + (\theta_c - \theta)}, \; W_M(F) \right\} & \text{for } \theta < \theta_c \end{cases} \quad (2.2)$$

for suitable constants $C_A, C_M \geq 1$. Notice that if $C_A = C_M = 1$, then both austenitic and martensitic local minima exist for all values of θ. However, if $C_A > 1$, then the martensitic variants U_i cease to be a local minimizer of $\phi(F, \theta, \theta_c)$ at $\theta = \theta_c + (C_A - 1)^{-1}W_A(U_1)$, that is, martensite becomes "unstable." Similarly, if $C_M > 1$, then the austenitic phase I ceases to be a local minimizer of $\phi(F, \theta, \theta_c)$ at $\theta = \theta_c - (C_M - 1)^{-1}W_M(I)$, that is, austenite becomes "unstable." In our computational model, we shall take $C_M = 1 + W_M(I)$ and either $C_A = 1$ or $C_A = 1 + W_A(U_1)$. Notice that for $C_M = 1 + W_M(I)$ or $C_A = 1 + W_A(U_1)$ the instability occurs at (scaled) temperatures $\theta - \theta_c = \pm 1$. Since we shall only study the transformation from martensite to austenite during heating in this paper, the choice of C_M is not important since it only concerns the instability of austenite at temperatures below the transformation temperature.

We note that the energy density ϕ is frame-indifferent. Since the martensitic energy density W_M is minimized only at the wells with the maximal in-plane extensions generated by the four variants U_i, $i = 1, \ldots, 4$, it has reduced tetragonal symmetry, while the austenitic energy density has the full cubic symmetry. Hence, the energy density ϕ has tetragonal symmetry.

3. Compositional Fluctuations

We next describe the form of the spatial fluctuation of the transformation temperature corresponding to a spatial fluctuation of the composition. As in [5], we shall assume that the temperature has been scaled so that (2.2) provides a model with good approximation of the (scaled) temperature dependence. Assuming that the crystal has a bulk composition c that corresponds to a mean transformation temperature $\bar{\theta}_c$ and assuming that the transformation temperature exhibits linear

dependence on the composition, we model the transformation temperature $\theta_c(x)$ by independent Gaussian random variables $\theta_c|_K$ indexed by the triangles K in the finite element mesh with mean $\bar{\theta}_c$ and standard deviation σ :

$$\langle \theta_c|_K \rangle = \bar{\theta}_c, \qquad \langle (\theta_c|_K - \bar{\theta}_c)(\theta_c|_{K'} - \bar{\theta}_c) \rangle = \sigma^2 \, \delta_{KK'}.$$

Thus, $\theta_c(x)$ is piecewise constant on the finite element triangulation, and we compute $\theta_c(x)$ on each triangle by a Gaussian pseudo-random number with mean $\bar{\theta}_c$ and standard deviation σ on each triangle. Without loss of generality, we will normalize the temperature scale so that mean transformation temperature $\bar{\theta}_c = 0$.

4. The Thin Film Model and Discretization

We next give a short description of the total-variation model for thin films of martensitic single crystal materials. This model has been rigorously derived by the authors in [6] following earlier work on a strain-gradient model by Bhattacharya and James [4].

For our total-variation surface energy model, the bulk energy for a film of thickness $h > 0$ with reference configuration $\Omega_h \equiv \Omega \times (-h/2, \, h/2)$, where $\Omega \subset \mathbb{R}^2$ is a domain with a Lipschitz continuous boundary $\partial\Omega$, is given by the sum of the surface energy and the elastic free energy

$$\kappa \int_{\Omega_h} |D(\nabla u)| + \int_{\Omega_h} \phi(\nabla u(x), \theta(x), \theta_c(x)) \, dx, \tag{4.1}$$

where $\int_{\Omega_h} |D(\nabla u)|$ is the total variation of the deformation gradient [5,6] and κ is a small positive constant. The total variation of a piecewise smooth deformation gradient ∇u that has discontinuities across the surfaces σ_j, $j = 1, \ldots, J$, separating the open sets ω_ℓ in the disjoint union $\Omega_h = \sum_{\ell=1}^{L} \omega_\ell$ is given by

$$\int_{\Omega_h} |D(\nabla u)| = \sum_{j=1}^{J} \int_{\sigma_j} |[\![\nabla u]\!]_{\sigma_j}| \, dS + \sum_{\ell=1}^{L} \int_{\omega_\ell} \sqrt{\sum_{m,n=1}^{3} \left(\frac{\partial^2 u(x)}{\partial x_m \partial x_n} \right)^2} \, dx,$$

where $|[\![\nabla u]\!]_{\sigma_j}|$ denotes the euclidean norm of the jump of the deformation gradient across the interface σ_j.

We assume the film to be bonded at $\partial\Omega \times (-h/2, \, h/2)$, so the admissible deformations are constrained by the boundary condition

$$u(x_1, x_2, x_3) = (x_1, x_2, x_3) \quad \text{for } (x_1, x_2) \in \partial\Omega, \ x_3 \in (-h/2, \, h/2).$$

We can more generally consider the boundary constraint

$$u(x_1, x_2, x_3) = y_0(x_1, x_2) + b_0(x_1, x_2)x_3 \quad \text{for } (x_1, x_2) \in \partial\Omega, \ x_3 \in (-h/2, \, h/2),$$

for fixed functions y_0, b_0.

If the energy density $\phi(F, \theta, \theta_c)$ is a continuous function satisfying the growth condition

$$c_1(|F|^p - 1) \leq \phi(F, \theta, \theta_c) \leq c_2(|F|^p + 1) \quad \text{for all } F \in \mathbb{R}^{3 \times 3} \text{ and } \theta, \theta_c \in (\theta_0, \theta_1), \tag{4.2}$$

where c_1 and c_2 are fixed positive constants and $p > 3$ to ensure that deformations with finite energy are uniformly continuous, then we can show [6] (for the case that the temperature fields θ and θ_c do not vary in space) that energy-minimizing deformations u of the bulk energy (4.1) are asymptotically of the form

$$u(x_1, x_2, x_3) = y(x_1, x_2) + b(x_1, x_2)x_3 + o(x_3^2) \quad \text{for } (x_1, x_2) \in \Omega, \ x_3 \in (-h/2, \, h/2), \tag{4.3}$$

where $(y, b) : \Omega \times \Omega \to \mathbb{R}^3 \times \mathbb{R}^3$ minimizes the thin film energy

$$\mathcal{E}(y, b; \theta, \theta_c) = \kappa \left(\int_\Omega |D(\nabla y | \sqrt{2}b)| + \sqrt{2} \int_{\partial\Omega} |b - b_0| \right) + \int_\Omega \phi(\nabla y(x) | b(x), \theta(x), \theta_c(x)) \, dx \quad (4.4)$$

over all pairs $(\tilde{y}, \tilde{b}) \in \mathcal{A}$ of finite energy such that $\tilde{y} = y_0$ on $\partial\Omega$. More precisely, the space of admissible deformations of the thin film is given by

$$\mathcal{A} = \{ (\tilde{y}, \tilde{b}) \in W^{1,p}(\Omega; \mathbb{R}^3) \times L^p(\Omega; \mathbb{R}^3) : \ \nabla\tilde{y}, \tilde{b} \in BV(\Omega), \ \tilde{y} = y_0 \text{ on } \partial\Omega \}.$$

The map b describes the deformation of the cross-section relative to the film [4]. We denote by $(\nabla y | b) \in \mathbb{R}^{3\times3}$ the matrix whose first two columns are given by the columns of ∇y and the last column by b and occasionally refer to it as the "deformation gradient." The integral $\int_\Omega |D(\nabla y | \sqrt{2}b)|$ is the total variation of the vector-valued function $(\nabla y | \sqrt{2}b) : \Omega \to \mathbb{R}^{3\times3}$.

As in [5], we shall use a finite element approximation to compute metastable states (local minima) of the energy functional (4.4). We shall assume that Ω is a polygonal domain and denote by τ a triangulation of Ω. We denote the (triangular) elements of τ by K and the inter-element and boundary edges by e. The internal edges of the triangulation will be denoted by $e \subset \Omega$ and the boundary edges by $e \subset \partial\Omega$. For an internal edge $e \subset \Omega$ and two elements $K_1, K_2 \in \tau$ sharing the edge e, we define the jump across the edge e of a function ψ by

$$[\![\, \psi \,]\!]_e = \psi_{e,K_1} - \psi_{e,K_2},$$

where ψ_{e,K_i} denotes the trace on e of $\psi|_{K_i}$ for $i = 1, 2$. The sign ambiguity in the definition of the jump will not cause an ambiguity in the description of the discrete energy below since only the euclidean norm of the jump is used. For a boundary edge $e \subset \partial\Omega$, we define $\psi|_e$ to be the trace of ψ on e.

We denote by $\mathcal{P}_1(\tau)$ the space of continuous, piecewise linear functions on Ω which are linear on each $K \in \tau$, and by $\mathcal{P}_0(\tau)$ the space of piecewise constant functions on Ω which are constant on each $K \in \tau$. For $(y, b) \in \mathcal{P}_1(\tau) \times \mathcal{P}_0(\tau)$ and $\theta, \theta_c \in \mathcal{P}_0(\tau)$, the energy (4.4) is well-defined, and we have that

$$\kappa \left[\int_\Omega |D(\nabla y | \sqrt{2}b)| + \sqrt{2} \int_{\partial\Omega} |b - b_0| \right] + \int_\Omega \phi(\nabla y(x) | b(x), \theta(x), \theta_c(x)) \, dx$$

$$= \kappa \left(\sum_{e \subset \Omega} \left| [\![\, (\nabla y | \sqrt{2}b) \,]\!]_e \right| |e| + \sqrt{2} \sum_{e \subset \partial\Omega} \left| b|_e - b_0|_e \right| |e| \right) + \sum_{K \in \tau} \phi(\nabla y | b, \theta, \theta_c)|_K) \, |K|,$$

where $|K|$ is the area of the element K and

$$\left| [\![\, (\nabla y | \sqrt{2}b) \,]\!]_e \right| = \left(\left| [\![\nabla y]\!]_e \right|^2 + 2 \left| [\![b]\!]_e \right|^2 \right)^{1/2}.$$

The above term is not differentiable everywhere, so we have regularized it in our numerical simulations.

5. METASTABLE INDENTATIONS

Bhattacharya and James [4] have shown that thin films of certain single-crystal martensitic alloys allow metastable tent-like indentations with a square base each of whose sides is predicted to consist of a single variant of martensite, with opposite sides consisting of the same, but rotated, variant. The square base does not change shape when the film transforms from austenite to martensite or vice versa, and hence the martensitic tent can be extended by undeformed austenite around the

tent. This allows the film to be attached to a substrate outside the square domain while being free to transform between a flat shape in the austenitic phase and a tent shape in martensitic phase.

We showed in [5] that for a slight change of the parameter δ to $\delta = \sqrt{(\alpha - 1)(\beta - 1)} \approx 0.0295$, there exists a metastable tent deformation of a square surface orthogonal to e_3 with a side parallel to $e \in \mathbb{R}^3$, $|e| = 1$, $e \cdot e_3 = 0$, along which that tent has deformation gradient $R(\chi, e)U_1$ in the martensitic phase and

$$
\begin{aligned}
&R(\chi, e)U_1 e = e, \\
&R(\chi, e)U_1 n \cdot R(\chi, e)U_1 e = U_1 n \cdot U_1 e = 0 \qquad \text{for } n = e_3 \times e, \\
&|R(\chi, e)U_1 n| = |U_1 n| > 1,
\end{aligned}
\tag{5.1}
$$

where $R(\chi, e)$ denotes the rotation of $\chi = \pm \arccos \lambda^{-1}$ radians about e and

$$
\begin{aligned}
e &= (\alpha + \beta - 2)^{-1/2} \left(\sqrt{\beta - 1}, \ -\sqrt{\alpha - 1}, \ 0 \right), \\
n &= (\alpha + \beta - 2)^{-1/2} \left(\sqrt{\alpha - 1}, \sqrt{\beta - 1}, \ 0 \right), \\
\lambda &= \frac{(\alpha + \beta) + \sqrt{(\alpha - \beta)^2 + 4\tilde{\delta}^2}}{2} = \frac{(\alpha + \beta) + \sqrt{(\alpha - \beta)^2 + 4(\alpha - 1)(\beta - 1)}}{2}.
\end{aligned}
\tag{5.2}
$$

Since $R(\pi/2, e_3)^T U_1 R(\pi/2, e_3) = U_4$, where $R(\pi/2, e_3) \in \mathrm{SO}(3)$ is the rotation of $\pi/2$ radians about e_3, we can conclude by symmetry that the other faces of the tent have deformation gradient $R(\chi, n)U_4$, $R(-\chi, e)U_1$, and $R(-\chi, n)U_4$. The height of the tent is given by

$$
\xi = \text{height of tent} = \frac{1}{4}\sqrt{\lambda^2 - 1} = \frac{1}{2}\sqrt{(\alpha + \beta)(\alpha + \beta - 2)}.
$$

6. The Computational Model

Computational results of the authors [5] simulated the experiment in [9]. In this paper, we will only focus on the second stage of the experiment, in which the tent is being heated by a water bath surrounding the part of the film that is attached to the substrate. In this stage, the film transforms from a tent-like martensitic shape to a flat austenitic shape as the heat diffuses into the film from the boundary. We reported simulations of a shrinking tent-like indentation in [5]. In the laboratory experiment of [9], the tent retained its sharp shape during the initial heating, but then the edges of the tent became rounded until the film eventually fully transformed to austenite. Our intent is to study the effect on the shape of the transforming film of compositional variation, spatial temporal noise, and the instability of the metastable phase in the free energy density sufficiently far from the transformation temperature.

As in the computational study [5], we utilize a quasi-static continuation technique, in which the temperature field evolves dynamically and in which the deformation field evolves quasi-statically by computing the local minimum of the energy (evaluated at the updated temperature field) with the initial guess given by the deformation field at the previous time step.

The temperature field $\theta(x, t)$ is modeled simply by

$$
\begin{aligned}
\theta_t(x, t) &= \mu \, \Delta\theta(x, t) &\text{for } (x, t) &\in \Omega \times (0, +\infty), \\
\theta(x, t) &= \theta_{\partial\Omega} &\text{for } (x, t) &\in \partial\Omega \times (0, +\infty), \\
\theta(x, 0) &= \theta_{\text{init}} &\text{for } x &\in \Omega,
\end{aligned}
\tag{6.1}
$$

where $\theta_{\text{init}} < \theta_c = 0$ is the constant initial temperature of the film. Here, μ is the diffusivity coefficient which we can take equal to 1 by scaling time.

In the computational experiments presented below, the temperature on the boundary is given by $\theta_{\partial\Omega} = 1$, and the temperature in the interior at the initial time is given by $\theta_{\text{init}} = -1$. The domain is given by $\Omega = (0,1) \times (0,1)$, and we set as in [5] the surface energy coefficient $\kappa = 4 \times 10^{-4}$. The heat equation for the thermal field $\theta(x,t)$ given by (6.1) is solved by evaluating the series given in [5].

Our space of approximate admissible deformations is given by

$$\mathcal{A}_\tau = \{(y,b) \in \mathcal{P}_1(\tau) \times \mathcal{P}_0(\tau) : \ y = y_0 \text{ on } \partial\Omega\}, \tag{6.2}$$

where

$$y_0(x) = (x_1, x_2, 0) \quad \text{for } x = (x_1, x_2) \in \partial\Omega,$$
$$b_0(x) = (0, 0, 1) \quad \text{for } x = (x_1, x_2) \in \partial\Omega.$$

We construct our finite element mesh by dividing the square computational domain $\Omega = (0,1) \times (0,1)$ into $N \times N$ congruent squares with sides of length $h = 1/N$. Each of these squares is further subdivided into four triangles by the diagonals of the square. The results will be presented on meshes with $N = 64$.

The time domain $[0,T]$ for $T > 0$ is partitioned by $0 = t_0 < t_1 < \cdots < t_{L-1} < t_L = T$. For the computations presented below in Figures 1, 3, and 4 a uniform time step of $t_\ell - t_{\ell-1} = 0.00025$ is used. The deformation $(y(t_\ell), b(t_\ell)) \in \mathcal{A}_\tau$ for $\ell = 0, \ldots, L$ is then obtained by computing a local minimum for the energy $\mathcal{E}(y, b; \theta(t_\ell), \theta_c)$ by the Polak-Ribière conjugate gradient method [14] with initial iterate

$$(y^{[0]}(t_\ell), b^{[0]}(t_\ell)) = (y(t_{\ell-1}), b(t_{\ell-1})) + (\delta y(t_\ell), \delta b(t_\ell)),$$

where random vibrations are modeled by $\delta y(t_\ell)$ and $\delta b(t_\ell)$. The components of $\delta y(t_\ell)$ at the nodes of the triangulation are computed by a Gaussian pseudo-random number generator with mean 0 and standard deviation $\alpha \frac{h}{\sqrt{2}}$, and the components of $\delta b(t_\ell)$ on the triangles are computed by a Gaussian pseudo-random number generator with mean 0 and standard deviation α. We note that since the values of the computed pseudo-random $\delta y(t_\ell)$ at the mesh points are independent, the standard deviation of the derivatives of $\delta y(t_\ell)$ are α and $\sqrt{3}\alpha$ depending on the orientation of the triangle. If the conjugate gradient iterations have converged to an acceptable tolerance after M iterations, we set

$$(y(t_\ell), b(t_\ell)) = (y^{[M]}(t_\ell), b^{[M]}(t_\ell)).$$

7. Numerical Results

In this section, we shall study the effect of spatial compositional fluctuation (which gives a spatial fluctuation to the transformation temperature), the addition of noise in space and time to the evolution of the deformation, and the loss of metastability of the martensitic phase at temperatures sufficiently above the transformation temperature ($C_A > 1$ in the energy density (2.2)). We set the initial data for our computation to be

$$(y^{[0]}(t_0), b^{[0]}(t_0)) = (y^{\text{tent}}, b^{\text{tent}}) + (\delta y(t_0), \delta b(t_0)),$$

where $(y^{\text{tent}}, b^{\text{tent}})$ denotes the tent deformation described in Section 5. We investigate how the compositional fluctuation and spatial-temporal noise effects whether the film transforms from the martensitic tent, the rate of the transformation, and the path of the transformation through its metastable states. We recall that in [5] we introduced a nucleation step into the algorithm because we observed that if martensite is a metastable state for the energy density at all temperatures ($C_A = 1$), then the martensitic tent will be a local minimum of the energy density and will not transform as the film is heated.
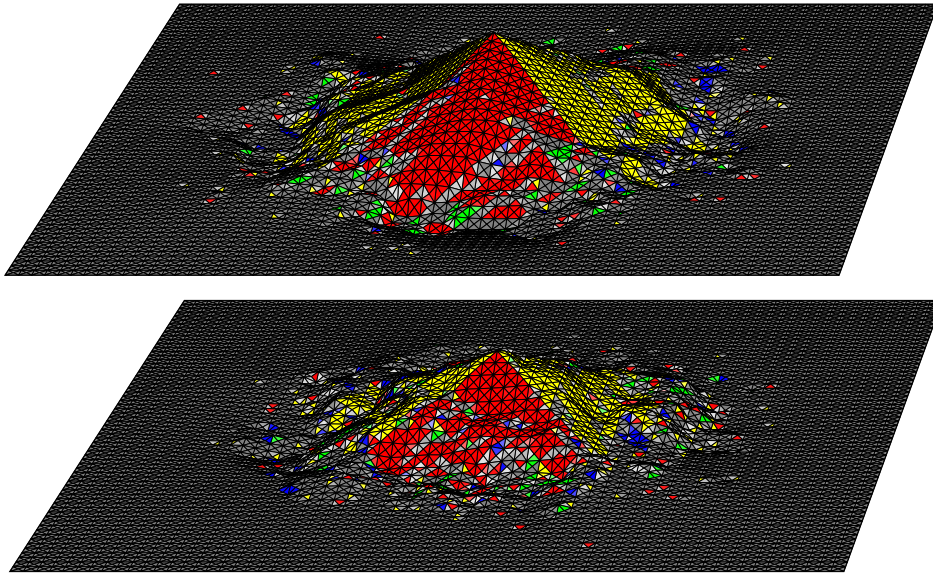
FIGURE 1. Top to bottom: Standard deviation in $\delta y(x_j, t_n) = 0.005h$, $0.01h$. Standard deviation in $\delta\theta_c \mid_K = 0.22$. No loss of metastability in energy density for $\theta \gg \theta_c$ and $\theta \ll \theta_c$.

We present in Figures 1, 3, and 4 computational results for the models described above at time $t = 0.06$. The figures show the mesh, the deformation $y(x_1, x_2)$, and the deformation gradient $(\nabla y|b)|_K$ on each element K. The deformation gradient $(\nabla y|b)|_K$ is exhibited by a coloring scheme whereby the coloring of the element is determined by the distance to the nearest phase or variant [12]. In our coloring scheme, elements near the austenitic phase $F = I$ are colored a shade of grey and elements near the martensitic variants are colored shades of red for $F = U_1$, shades of blue for $F = U_2$, shades of green for $F = U_3$, and shades of yellow for $F = U_4$.

If noise is added to the deformation ($\alpha > 0$), then there is a nonzero probability that the noise $(\delta y(t_\ell), \delta b(t_\ell))$ added to the deformation at any time step will transform

$$(y^{[0]}(t_\ell), b^{[0]}(t_\ell)) = (y(t_{\ell-1}), b(t_{\ell-1})) + (\delta y(t_\ell), \delta b(t_\ell))$$

to a global minimum of the energy $\mathcal{E}(y, b; \theta, \theta_c(t_\ell))$ without the inclusion of a nucleation step in the algorithm or modifications of the energy density for compositional fluctuation or metastability. For this reason, we can conclude that the film will always eventually transform from the martensitic tent to the austenitic plate if $\theta_{\partial\Omega} > \theta_c$ and some spatial-temporal noise is added to the deformation ($\alpha > 0$). As expected, we found in our computations that the transformation proceeded more quickly with increasing noise (increasing α) and that the indentation was more rounded (see Figure 1).

If there is no loss of metastability of martensite at any temperature ($C_A = 1$), no noise is added to the deformation ($\alpha = 0$), and there is no surface energy $\kappa = 0$, then the martensitic tent will be a local minimum of the energy $\mathcal{E}(y, b; \theta, \theta_c(t_\ell))$ for any spatial fluctuation of the transformation temperature $\theta_c(x)$ and will not transform to austenite even at high temperatures.

However, for positive surface energy $\kappa > 0$ and positive standard deviation σ of the transformation temperature $\theta_c(x)$, there is nonzero probability that the energy-decreasing iteration with initial state given by the martensitic tent will evolve to the flat austenitic state. To see this, we define a continuous family of tents parametrized by $\mu \in [0, 1]$ such that $(y^{\mu,\text{tent}}(x), b^{\mu,\text{tent}}(x))$ is the

martensitic tent deformation described in Section 5 for $\mu = 1$ and is the austenitic plate deformation $y(x_1, x_2) = (x_1, x_2, 0)$, $b = (0, 0, 1)$ for $\mu = 0$. We define $y^{\mu, \text{tent}}(x)$ to be the tent with height $\mu \xi$ where ξ is the height of the martensitic tent described in Section 5, and

$$b^{\mu, \text{tent}}(x) = (1 - \mu)e_3 + \mu b^{\text{tent}}(x).$$

Since we assume here that the standard deviation in the transformation temperature is positive ($\sigma > 0$), there is a nonzero probability that $\theta_c(x)$ will be constant (to make things simple) and that $\theta_{\text{init}} - \theta_c > 0$ will be arbitrarily large. We will prove that for $\theta_{\text{init}} - \theta_c > 0$ sufficiently large, we have that

$$\mathcal{E}(y^{\mu, \text{tent}}, b^{\mu, \text{tent}}; \theta_{\text{init}}, \theta_c)$$

is a strictly increasing function for μ varying between $\mu = 0$ and $\mu = 1$. We can prove this by obtaining from direct calculation that

$$\int_\Omega |D(\nabla y^{\mu, \text{tent}} | \sqrt{2} b^{\mu, \text{tent}})| = 2\sqrt{2}\mu \sqrt{8\xi^2 + \frac{2\gamma^2}{1 + (4\xi)^2}},$$

and that we can choose $0 \le \mu_1 < 1$ such that

$$\int_\Omega |D(\nabla y^{\mu, \text{tent}} | \sqrt{2} b^{\mu, \text{tent}})| + \int_\Omega W_M(\nabla y^{\mu, \text{tent}}(x) | b^{\mu, \text{tent}}(x)) \, dx$$

is strictly increasing in $[\mu_1, 1]$ since the tent deformation $\mu = 1$ minimizes the martensitic elastic energy

$$\int_\Omega W_M(\nabla y(x) | b(x)) \, dx$$

in the set of admissible deformations $\mathcal{A}$ (see Figure 2). The proof that $\mathcal{E}(y^{\mu, \text{tent}}, b^{\mu, \text{tent}}; \theta_{\text{init}}, \theta_c)$ is a strictly increasing function for μ varying between $\mu = 0$ and $\mu = 1$ follows from the observation that for sufficiently large $\theta_{\text{init}} - \theta_c$ we have that $(\nabla y^{\mu, \text{tent}}(x) | b^{\mu, \text{tent}}(x))$ is in the austenitic energy well for $\mu \in [\mu_1, 1]$ (see Figure 2), and hence the elastic energy density (2.2) is given by $\phi(\nabla y^{\mu, \text{tent}}(x) | b^{\mu, \text{tent}}(x), \theta_{\text{init}}(x), \theta_c(x)) = W_A(\nabla y^{\mu, \text{tent}}(x) | b^{\mu, \text{tent}}(x))$. Thus,

$$\int_\Omega \phi(\nabla y^{\mu, \text{tent}}(x) | b^{\mu, \text{tent}}(x), \theta_{\text{init}}(x), \theta_c(x)) \, dx$$

is also increasing for $\mu \in [0, \mu_1]$.

We see in Figure 3 that if the martensitic phase ceases to be a metastable state at $\theta = \theta_c + 1 = 1$ ($C_A = 1 + W_A(U_1)$) and if positive standard deviation ($\sigma > 0$) in the transformation temperature is included in the model, then there is a nonzero probability that the film will transform from the martensitic tent to the austenitic plate even if no noise is added to the deformation ($\alpha = 0$). We note that the martensite will not be stable at a time t_ℓ and on an element $K \in \tau$ for which $\theta(x, t) > \theta_c|_K + 1 = 1$. The transformation proceeds more quickly and the tent rounds more as the standard deviation in the transformation temperature, σ, is increased.

We finally present computational results when martensite remains a metastable phase for all temperatures ($C_A = 1$) and spatial-temporal noise $\alpha > 0$ is added to the deformation. We find in Figure 4 that the transformation proceeds more quickly and the tent rounds more as the standard deviation in the transformation temperature, σ, is increased.
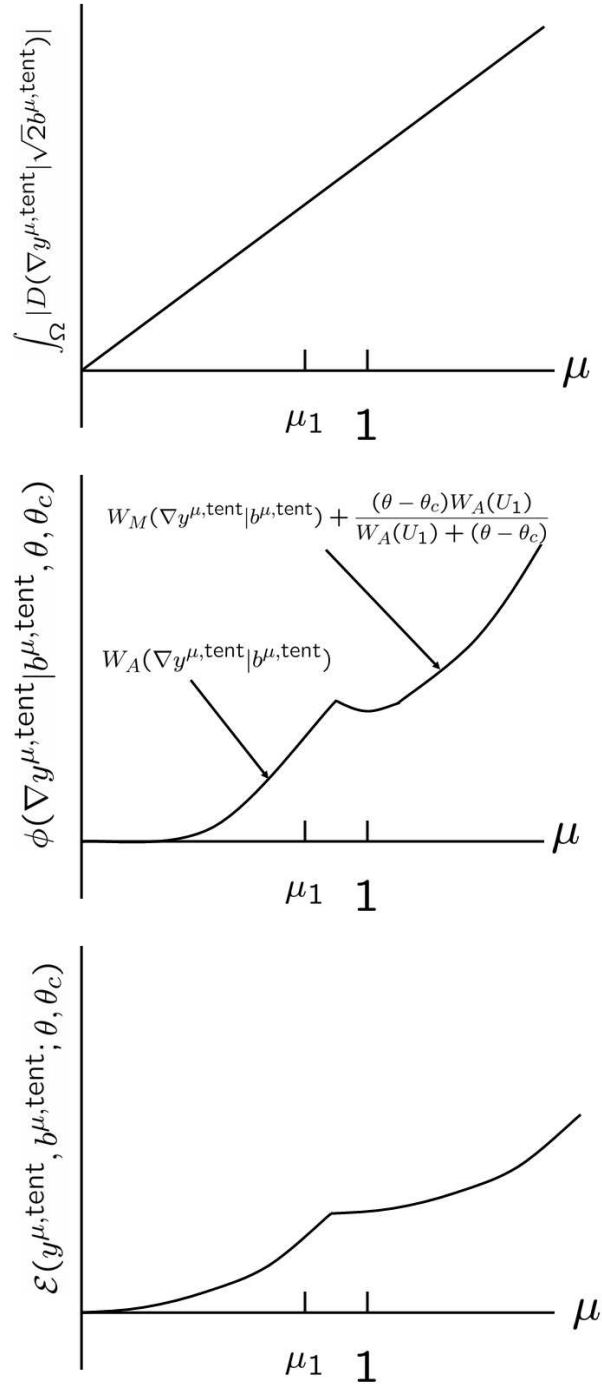
FIGURE 2. The dependence of $\int_\Omega |D(\nabla y^{\mu,\text{tent}}|\sqrt{2}b^{\mu,\text{tent}})|$, $\phi(\nabla y^{\mu,\text{tent}}|b^{\mu,\text{tent}}, \theta, \theta_c)$, and $\mathcal{E}(y^{\mu,\text{tent}}, b^{\mu,\text{tent}}; \theta, \theta_c)$ on μ for $\theta - \theta_c$ sufficiently large.
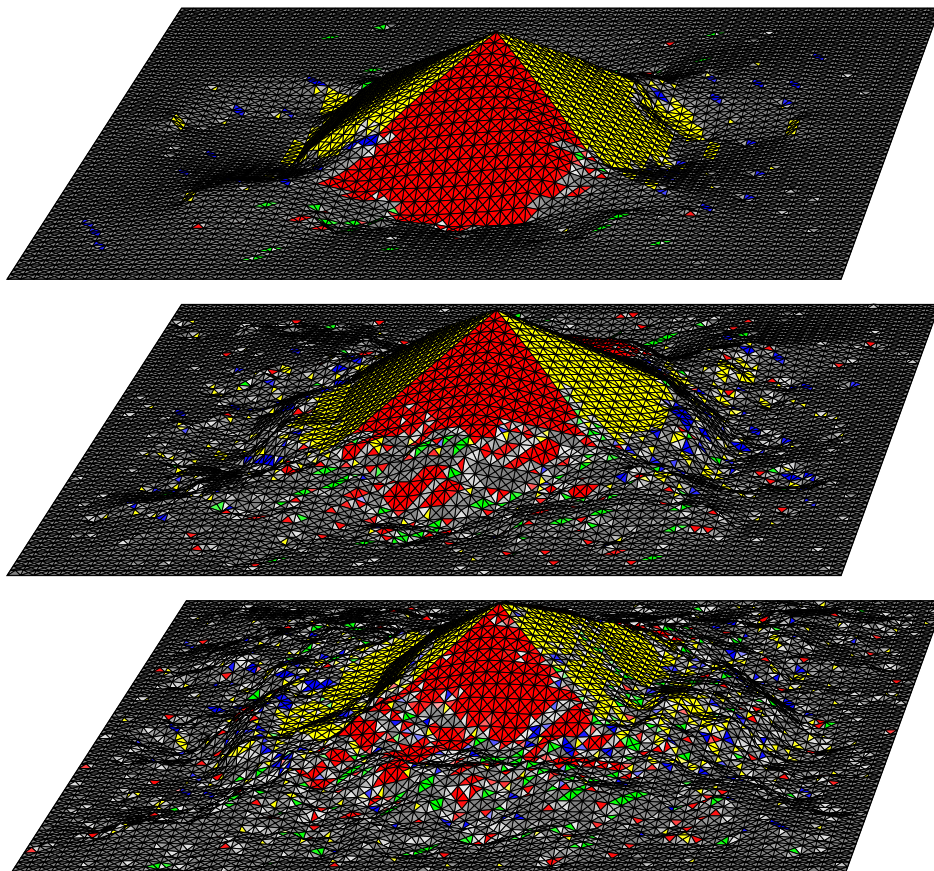
FIGURE 3. Top to bottom: Standard deviation in $\delta\theta_c \mid_K = 0.11$, 0.22, 0.33. No noise, so $\delta y(x_j, t_n) = 0$. Loss of metastability of martensite at $\theta = \theta_c + 1 = 1$.

REFERENCES

[1] John M. Ball and Richard D. James, Fine phase mixtures as minimizers of energy, *Arch. Rat. Mech. Anal.* **100** (1987) 13–52.

[2] John M. Ball and Richard D. James, Proposed experimental tests of a theory of fine microstructure and the two-well problem, *Phil. Trans. R. Soc. Lond. A.* **338** (1992) 389–450.

[3] Kaushik Bhattacharya and Georg Dolzmann, Relaxed constitutive relations for phase transforming materials, *J. Mech. Phys. Solids.* **48** (2000) 1493–1517.

[4] Kaushik Bhattacharya and Richard D. James, A theory of thin films of martensitic materials with applications to microactuators, *J. Mech. Phys. Solids.* **47** (1999) 531–576.

[5] Pavel Bělík and Mitchell Luskin, A computational model for the indentation and phase transformation of a martensitic thin film, *J. Mech. Phys. Solids.* **50** (2002) 789–1815.

[6] Pavel Bělík and Mitchell Luskin, A total-variation surface energy model for thin films of martensitic crystals, *Interfaces and Free Boundaries.* **4** (2002) 71–88.

[7] S. Chakravorty and C. M. Wayman, Electron microscopy of internally faulted Cu-Zn-Al martensite, *Acta. Metall.* **25** (1997) 989–1000.

[8] S.-Y. Chu, R. Gallager, M. De Graef, and M. E. McHenry, Structural and magnetic phase transitions in Ni-Mn-Ga ferromagnetic shape-memory crystals, *IEEE Transactions on Magnetics.* **37** (2001) 2666–2668.

[9] Jun Cui and Richard D. James, A "tent" shape thermoelastic deformation on foil of CuAlNi single crystal. Manuscript (2000).
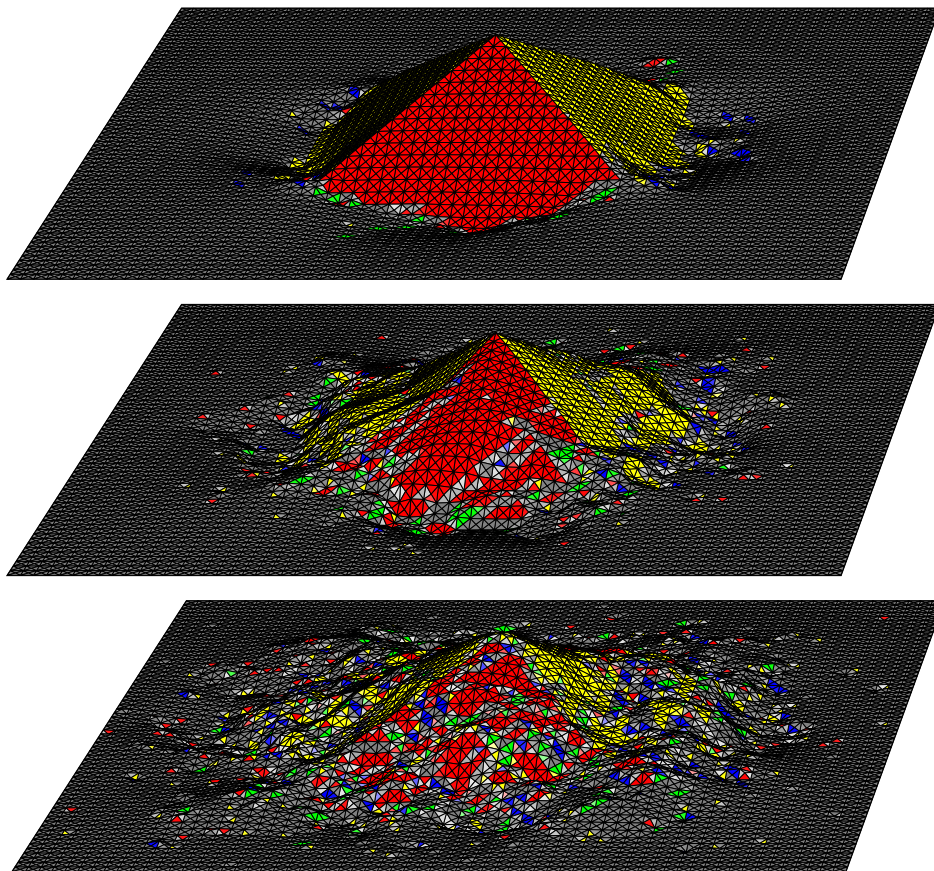
FIGURE 4. Top to bottom: Standard deviation in $\delta\theta_c \mid_K = 0.11, 0.22, 0.33$. Standard deviation in $\delta y(x_j, t_n) = 0.005h$. No loss of metastability in energy density for $\theta \gg \theta_c$ and $\theta \ll \theta_c$.

[10] J.W. Dong, J.Q. Xie, J. Lu, C. Adelmann, C.J. Palmstrøm, J. Cui, Q. Pan, T.W. Shield, R.D. James, and S. McKernan, Shape memory and ferromagnetic shape memory effects in single-crystal Ni_2MnGa thin films, *J. Appl. Phys.* **95** (2004) 2593–2600.

[11] Sivan Kartha, James A. Krumhansl, James P. Sethna, and Lisa K. Wickham, Disorder-driven pretransitional tweed in martensitic transformations, *Phys. Rev. B.* **52** (1995) 803–822.

[12] Mitchell Luskin, On the computation of crystalline microstructure, *Acta Numerica.* **5** (1996) 191–258.

[13] Mitchell Luskin, Computational modeling of microstructure, In *Proceedings of the International Congress of Mathematicians, ICM 2002, Beijing*, volume III, (2002) 707–716.

[14] Jorge Nocedal and Stephen Wright, *Numerical Optimization* (Springer-Verlag, 1999).

[15] A. N. Vasil'ev, A. D. Bozhko, V. V. Khovailo, et al, Structural and magnetic phase transitions in shape-memory alloys $Ni_{2+x}Mn_{1-x}Ga$. *Phys. Rev. B.* **59** (1999) 1113–1120.

PAVEL BĚLÍK, DEPARTMENT OF MATHEMATICS, UNIVERSITY OF ST. THOMAS, 2115 SUMMIT AVENUE, ST. PAUL, MN 55105, U.S.A.
  E-mail address: `pbelik@stthomas.edu`

MITCHELL LUSKIN, SCHOOL OF MATHEMATICS, UNIVERSITY OF MINNESOTA, 206 CHURCH STREET SE, MINNEAPOLIS, MN 55455, U.S.A.
  E-mail address: `luskin@math.umn.edu`